applied sciences

MDPI

Article

Odor Impact Assessment via Dispersion Model: Comparison of Different Input Meteorological Datasets

Francesca Tagliaferri [1], Laura Facagni [1], Marzio Invernizzi [1,*], Adrian Luis Ferrer Hernández [2], Anel Hernández-Garces [3] and Selena Sironi [1]

[1] Department of Chemistry, Materials and Chemical Engineering "Giulio Natta", Politecnico di Milano, Piazza Leonardo da Vinci 32, 20133 Milan, Italy; francesca.tagliaferri@polimi.it (F.T.); laura99facagni@gmail.com (L.F.); selena.sironi@polimi.it (S.S.)
[2] Center for Atmospheric Physics, Meteorology Institute (INSMET), Loma de Casablanca, Regla, Havana 11700, Cuba; adrian.ferrer@insmet.cu
[3] Faculty of Chemical Engineering, Universidad Tecnológica de La Habana José Antonio Echeverría, Calle 114, No. 11901. e/Ciclovía y Rotonda, Marianao, Havana 19390, Cuba; anel@quimica.cujae.edu.cu
* Correspondence: marzio.invernizzi@polimi.it

Abstract: Dispersion modeling is a useful tool for reproducing the spatial–temporal distribution of pollutants emitted by industrial sites, particularly in the environmental odor field. One widely used tool, accepted by regulatory agencies for environmental impact assessments, is the CALPUFF model, which requires a large number of input variables, including meteorological and orographical variables. The reliability of model results depends on the accuracy of these input variables. The present research aims to discuss a comparative study of odor dispersion modeling by initializing the CALMET meteorological processor with different input data: surface and upper air observational meteorological data, 3D prognostic data, and a blend of prognostic and measured data. Two distinct sources (a point and an area source) and two different simulation domains in Cuba and Italy are considered. The analysis of results is based on odor impact criteria enforced in some Italian regions by computing the 98th percentile of odor peak concentrations on an annual basis. For the area source, simulation results reveal that the 'OBS' and 'HYBRID' modes are largely comparable, whereas prognostic data tend to underestimate the odor concentrations, likely due to a reduced percentage of wind calms. For point sources, different input meteorological settings provide comparable results, with no significant differences.

Keywords: dispersion modeling; CALPUFF model; odor impact assessment; intercomparison; WRF; meteorological data

Citation: Tagliaferri, F.; Facagni, L.; Invernizzi, M.; Ferrer Hernández, A.L.; Hernández-Garces, A.; Sironi, S. Odor Impact Assessment via Dispersion Model: Comparison of Different Input Meteorological Datasets. *Appl. Sci.* **2024**, *14*, 2457. https://doi.org/10.3390/app14062457

Academic Editor: Jiangjun Wei

Received: 13 February 2024
Revised: 7 March 2024
Accepted: 12 March 2024
Published: 14 March 2024

1. Introduction

Due to rapid population and industrial growth in recent decades, the number of contaminants released into the atmosphere is rapidly growing [1,2]. In this context, complaints about annoyance due to environmental odors, typically emitted by industrial and agricultural activities, are a common way for people to express dissatisfaction to authorities [3–5]. Determining the extent of chemical exposure, particularly odor [6], becomes a crucial concern as we learn more about atmospheric pollution and its effects on citizens' health, the ecosystem, and well-being [7,8].

Odors are currently monitored and regulated in many nations [9]. The need to control odor impacts involves the development and application of specific methods to assess ground-level odor concentration [4,10–13]. In this sense, dispersion modeling is a valuable technique for replicating the spatial–temporal distribution of contaminants released by a single source to estimate areas of population exposure as well as ground-level concentrations of contaminants [14–22].

The Lagrangian Gaussian puff model CALPUFF, listed by the U.S. Environmental Protection Agency (EPA) as an alternative model for assessing the near-field transport of pollutants, has been widely used and accepted by regulatory agencies for environmental impact assessments [23]. In the CALMET/CALPUFF modeling system, the meteorological pre-processor CALMET is used to produce 3D meteorological data (e.g., wind and temperature fields) through advanced elaborations of available surface and upper air measurements, prognostic data from meso-scale models (e.g., WRF model), and geophysical data [24–26].

The trustworthiness of dispersion models is influenced by various sources of uncertainty. First, the dispersion model and its parametrizations (e.g., internal model parameters, dispersion parameterizations, deposition, etc.) are important sources of uncertainty. Moreover, different studies focus on models' sensitivity [6,23,27–29], highlighting the influence of different parameters (e.g., stack temperature, source diameter) related to the emission source. Another significant source of uncertainty is represented by the input meteorological data used to run the simulations.

Indeed, the dispersion of pollutants in the atmosphere is intricately linked to various meteorological parameters. Wind speed and direction play a significant role in determining the transport of pollutants. Higher wind speeds facilitate the dispersion of pollutants over larger distances, while wind direction determines the trajectory and potential impact areas. Atmospheric stability is another critical factor. Under stable conditions, where the air near the surface is cooler and denser than aloft, pollutants may be trapped near the ground, leading to higher concentrations and localized pollution hotspots. In contrast, unstable conditions promote vertical mixing, allowing pollutants to disperse more evenly throughout the atmosphere. Temperature and humidity also influence pollutant dispersion. Temperature inversions, where warmer air sits above cooler air near the surface, can hinder vertical mixing and trap pollutants beneath the inversion layer. Humidity affects the solubility of pollutants and can influence their removal from the atmosphere through processes like wet deposition.

Until now, the existing literature has documented some studies about the influence of the choice of meteorological data on atmospheric dispersion for classical pollutants [30,31], revealing that atmospheric model predictions are significantly over/underestimated depending on the choice of input meteorological settings. However, as far as an odor impact assessment is concerned, to the best knowledge of the authors, only one study partially addresses this topic [32]. Murguia et al. [32] evaluated the effect of three different meteorological inputs on odor impact while considering a single type of source. The results of this paper emphasize the need for additional research to better analyze the influence of different prognostic weather models, such as MM5 and WRF models. Moreover, considering that CALPUFF has been widely used in the field of odor and accepted by regulatory agencies for environmental impact assessments, permitting, and compliance purposes, it is important to assess how the choice of meteorological data may affect simulated odor impact maps.

In view of this, the present research discusses a comparative study of the results of odor dispersion modeling by initializing the CALMET meteorological processor with different input data: surface and upper air observational meteorological data, 3D prognostic meteorological data, and blended prognostic and measured data. These configurations will be referred to as CALPUFF "OBS" (surface and upper air meteorological observations), CALPUFF "NO-OBS" (WRF prognostic model for surface and upper air data), and CALPUFF "HYBRID" (wind fields generated by CALMET with blended prognostic and measured meteorological data).

Odor exposure levels are simulated with each input meteorological setting for two different types of emission sources: a point source (i.e., a conveyed emission from an odor emission abatement system) and an area source (i.e., a wastewater tank), both in Italian and Cuban domains. The results are analyzed according to the Regional Guideline of Lombardy [33], which prescribes the computation of the 98th percentile of odor peak concentration values on an annual basis. Despite the absence of a universal approach for

defining short-term peak concentration, a constant factor of 2.3, to be multiplied by the hourly average concentration returned from the model, is suggested [33]. Due to the lack of a technical standard in Cuba in the field of odor, the aforementioned criterion has been considered in the current work for both Cuban and Italian domains.

In summary, the purpose of this study is to compare the results of odor dispersion modeling by implementing three different input meteorological settings (i.e., CALPUFF "NO-OBS", CALPUFF "OBS", and CALPUFF "HYBRID") in two different simulation domains (northern Italy and Cuba) for two different types of emission sources.

The novelty of this research is mainly related to the pollutant simulated. Indeed, in the case of "traditional" contaminants, concentrations are typically post-processed based on average or maximum concentrations. However, with odor, the main peculiarity compared to classical pollutants is that to characterize the instantaneous perception of the human nose, it is necessary to refer to short-term peak concentrations. Further details can be found in Invernizzi et al. (2020) [23]. Additionally, to the best of the authors' knowledge, this is the first investigation on the subject with two kinds of sources characterized by different emission mechanisms, exploring how they can be influenced by meteorology in different ways.

Finally, the implementation of two distinct simulation domains provides a broad perspective on the research. Despite similar orography, these two domains have very different typical meteorological conditions: Cuba is characterized by a tropical climate with high temperatures and abundant rainfall year-round, while the investigated Italian region (i.e., Po Valley) has a temperate climate with moderate temperatures. Precipitation in Cuba is frequent and intense, particularly during the monsoon season, whereas precipitation in the Po Valley is more evenly distributed throughout the year with seasonal variations. Temperature variations are more pronounced in the Po Valley, with distinct seasonal changes, compared to Cuba, where temperatures are more consistent throughout the year. The typical climate of the Po Valley is characterized by low winds, which are particularly weak in the winter months; winds in Cuba are often more intense, with extreme weather phenomena such as hurricanes that are quite common. In addition, the presence of a land–water interface in the Cuban domain (absent in the Italian one) may affect pollutant dispersion by influencing wind dynamics, coastal currents, and local thermal effects, such as sea and land breezes. These interactions play a significant role in the simulation of pollutant dispersion.

The structure of the paper includes a brief overview of CALMET and CALPUFF theories and a discussion about meteorological and emissive input data provided to the model (Section 2). Section 3 reports the results (simulated odor impact maps and separation distances) and provides a critical discussion. Finally, Section 4 summarizes the conclusions and possible future improvements.

2. Materials and Methods

2.1. CALPUFF

CALPUFF is a non-steady-state Lagrangian Gaussian puff model [34] in which individual puffs of pollutants are released and allowed to grow horizontally and vertically, spreading outward from the plume's centerline, following a normal statistical distribution, according to the following equations [34]:

$$C(x,y,z)=\frac{Q}{2\pi\sigma_x\sigma_y}g\left[exp\left(-\frac{1}{2}\left(\frac{d_a}{\sigma_x}\right)^2\right)\right]\left[exp\left(-\frac{1}{2}\left(\frac{d_c}{\sigma_y}\right)^2\right)\right] \quad (1)$$

$$g=\frac{2}{\sigma_z\sqrt{2\pi}}\sum exp\left[\frac{-(H_e+2nh)^2}{2\sigma_z^2}\right] \quad (2)$$

where C [g/m^3] is the concentration at (x, y, z) location; Q [g] is the mass of pollutant in the puff; σ_x, σ_y, and σ_z [m] are the Gaussian distribution standard deviations in the along-wind,

cross-wind, and vertical directions; d_a and d_c [m] are the distances from the puff barycenter to the receptor in the along-wind and cross-wind directions; H_e [m] is the height of the puff barycenter with respect to the ground; and h [m] is the mixing-layer height.

The Lagrangian puff formulation simulates the plume as a sequence of Gaussian puffs that move and disperse into the atmosphere in response to time and space-varying local conditions. The US-EPA [35] recommends CALPUFF as an alternative model for near-field transport (i.e., <50 km), as it contains modules of algorithms for complex topography, overwater dispersion, building downwash, wet and dry deposition, and chemical reactions. Moreover, CALPUFF, unlike traditional Gaussian plume models, is also able to simulate calm wind conditions, which is crucial for estimating odor impact: this condition is characterized by a low capacity of the atmosphere to disperse pollutants, making the occurrence of odor events likely.

In fact, the US-EPA recognizes that CALPUFF [36], compared to the preferred model AERMOD or other Gaussian plume models, may be more appropriate in specific situations (e.g., in the case of complex topography).

Furthermore, CALPUFF has been widely used and accepted by regulatory agencies for environmental impact assessments, permitting, and compliance purposes. It has a well-established user base and a history of regulatory acceptance in many jurisdictions.

The model is coupled with the meteorological processor CALMET, which provides 3D diagnostic wind and temperature fields for a CALPUFF dispersion simulation.

2.2. CALMET

As a diagnostic meteorological model, CALMET can reconstruct the wind field over a simple or complex orographic domain from ground measurements and at least one vertical profile [37,38]. It includes algorithms for computing planetary boundary layer meteorological parameters on land and water. These characteristics make it suitable for generating input for atmospheric dispersion models, which require both the mean wind field and an accurate description of turbulence via micrometeorological parameters.

2.2.1. Meteorological Data

The collection and preprocessing of meteorological data are of fundamental importance for environmental impact assessment studies [39]. The detail and quality of the input data requirements depend on the complexity of the model. Sophisticated, non-steady-state models—such as Lagrangian puff models like the CALPUFF/CALMET modeling system—can process a 3D dataset of meteorological data.

In principle, meteorological data could be obtained from meteorological stations (surface + upper air) or from prognostic models. The implementation of prognostic data appears to be necessary in certain locations where nearby meteorological stations are not available.

In this study, WRF prognostic data (CALPUFF "NO-OBS") as well as observational data, i.e., one surface station and one upper air station (CALPUFF "OBS"), are both implemented as input meteorological data to run the simulations. Additionally, CALPUFF "HYBRID" combines surface observational data and upper air prognostic data.

The meteorological prognostic data adopted for CALPUFF "NO-OBS" and CALPUFF "HYBRID" are 3D hourly data processed by the WRF (Weather Research and Forecasting) model with a spatial resolution of 1 km and 3 km, respectively, for the Italian and Cuban domains for the reference year 2016. For the Italian domain, the WRF data are collected by "Lakes Environmental", while the Cuban ones are processed by the "Centre for Atmospheric Physics" (Meteorology Institute of Cuba). The WRF configuration adopted in this study is based exclusively on analysis data from the Global Forecast System (GFS) model, meaning that no meteorological observation data were incorporated using any data assimilation method into the model.

Consistently, for the observed data, surface and upper air measurements from meteorological stations were considered for the same reference year for both the Cuban and Italian

domains. The reference year (i.e., 2016) was chosen as the most recent year with a complete meteorological dataset available for both domains. In both domains, the simulation period covers the entire year of 2016.

For the Cuban site, hourly surface meteorological observations for wind speed (Ws), wind direction (Wd), atmospheric pressure (Patm), air temperature (T), relative humidity (RH), and cloud cover (CC) were measured by the surface station Aguada de Pasajeros AGP, Cienfuegos (22.37° N, 80.83° W), located in the eastern part of the domain. The height of the meteorological station is 10 m above ground level.

To fulfill the standard quality criteria set by the CALMET meteorological pre-processor [38], upper air data were obtained from the upper station located in Key West KW, Florida, positioned about 240 km away from the domain (24.55° N, 81.75° W) due to the limited raw-insonde data available in this region. Despite this station being located more than 200 km away, numerous authors have used these data to represent the upper air in Cuba [40,41] based on the reports of Gandin [42] and Kitchen [43], who assert that upper air observations separated by distances of up to 2000 km and 1000 km, respectively, can be assumed without any notable error.

For the Italian site, hourly surface meteorological observations of Wd, Ws, T, Patm, and RH were acquired by the Regional Agency for Environmental Protection (ARPA Lombardia, Milan, Italy) for the station of Landriano Cascina Marianna LDR (45.32° N, 9.27° E), located inside the domain, in the same position as the Cuban surface station with respect to the corresponding SW corner. The height of the meteorological station is 10 m, as is the case for the monitoring station in Cuba. The measuring network of ARPA Lombardia does not provide CC data. Instead, the CC was obtained from the METAR meteorological database of Iowa State University for the station of Milano Linate International Airport LIML (45.43° N, 9.28° E), 13 km away from the domain.

The upper air meteorological data for the Italian domain were acquired from the NOAA/ESRL Radiosonde Database, particularly, from Milano Linate International Airport LIML (45.43° N, 9.28° E), 13 km away from the source. Table 1 summarizes the meteorological input data adopted to run the simulations.

Table 1. Meteorological stations selected for dispersion simulation.

Site	Station Acronym	Type	Coordinates	Elevation ASL [m]	Distance Met Station–Domain Center [km]
Italy	LDR	Surface	45.32° N, 9.27° E	88	2
Italy	LIML	Upper	45.43° N, 9.28° E	101	13
Cuba	AGP	Surface	22.37° N, 80.83° W	24	2
Cuba	KW	Upper	24.55° N, 81.75° W	6	240

To handle possible invalid or missing data obtained from measurement stations, the approach suggested by the US-EPA protocol [35] was adopted as a reference. In particular, this document recommends various substitution procedures (e.g., persistence, interpolation, profiling) depending on the nature of the application, the availability of alternative sources of meteorological data, and the extent of the missing or invalid data. In this study, the interpolation procedure is adopted to replace missing data.

2.2.2. CALMET Parameters

To run CALMET simulations, US-EPA-recommended parameter values [44] or CALMET default values were generally adopted, if available. However, the definition of model parameters for TERRAD, BIAS, R1, R2, RMAX1, and RMAX2 is mandatory (at least for CALPUFF "OBS" mode), but no default values or clear suggestions are provided in the Model User's Guide. The adopted values for these parameters are reported in Table 2. The rationale behind the selection of these numerical values will be briefly discussed, with the purpose of identifying the optimal configuration for CALMET settings.

Table 2. Input parameters for CALMET set-up.

Parameters		
TERRAD Italy	3	[km]
TERRAD Cuba	0.1	[km]
R1	5.7	[km]
R2	8.5	[km]
RMAX1	11.4	[km]
RMAX2	17	[km]
BIAS (for each vertical layer)	−1, −0.67, −0.33, 0, 0.2, 0.4, 0.6, 0.8, 1, 1	

TERRAD identifies the influence radius of terrain features and is required to run CALMET simulations for all the investigated input meteorological settings [38]. A sensitivity analysis with different TERRAD parameters was conducted to find the optimal value to minimize the Root Mean Square Error (RMSE) of the wind speed by comparing the "NO-OBS" CALMET output values with the observed measurements following [45]. Due to the flat orography of both domains (i.e., Italy and Cuba), RMSE values resulting from simulations with different TERRAD parameters were very similar. Through an optimum analysis, TERRAD was set to 3 km and 0.1 km for the Italian and Cuban domains, respectively.

The BIAS parameter, required only in the "OBS" and "HYBRID" mode, determines the relative weight associated with the surface measurements versus upper air data in the computation of the initial guess wind field [38]. By setting BIAS to −1, upper-air observations are not taken into account in the interpolations for this layer. Conversely, by setting BIAS to +1, surface observations are not considered in the interpolations for this layer.

One hundred percent of the weight (BIAS = −1) is attributed to surface meteorological data in the first vertical layer. These data have 0% weight in the last two layers (BIAS = 1). As recommended by Rzeszutek [37] and Rood [39], the same weight was assigned to the fourth layer (BIAS = 0), with a gradient of weights between the lower and upper for the remaining levels.

For "OBS" and "HYBRID" simulations, R1 and R2 must be set as well [38]. They represent the weight of each meteorological station inside the domain in the computation of the wind field. In the current study, due to the availability of only one station (one for surface and one for upper air), these parameters must cover the entire domain [46].

For this reason, R1, referring to the surface layer, was chosen as the greatest distance from the station to the domain's farthest point, i.e., 5.7 km. For R2, referring to upper layers, the diagonal of the domain was selected, i.e., 8.5 km, considering that selected upper air stations are located outside the corresponding domain (i.e., 13 km from the source for the Italian domain and 240 km for the Cuban domain). The values of these parameters are the same in the two simulations because the domains have identical dimensions, and the surface stations are positioned identically relative to their respective southwest corners.

RMAX1 and RMAX2 parameters, required for the "OBS" and "HYBRID" simulations, identify the maximum radius of influence for surface and upper data, respectively. According to the scientific literature, it is suggested to set these parameters equal to twice R1 and R2 [47]. Therefore, a value of 11.4 km was selected for RMAX1 and 17 km for RMAX2.

2.3. Site Domain

The simulation domains for Italy and Cuba have the same dimension, 6 km × 6 km with a grid resolution of 100 m. Indeed, CALPUFF is frequently used, in the field of odor, for short-range scales with simulation domains smaller than 10 km × 10 km [23,29].

Ten vertical layers are defined with the vertical heights of 20, 40, 80, 160, 320, 640, 1200, 2000, 3000, and 4000 m, giving a total number of cells in the domain equal to 36,000.

The Italian simulation domain is situated south of Milan (SW corner: 45.29° N, 9.21° E). The Cuban domain is located in the central part of Cuba, northwest of Cienfuegos (SW corner: 22.35° N, 80.87° W). Figure 1 shows the location of the two domains in Italy and Cuba.

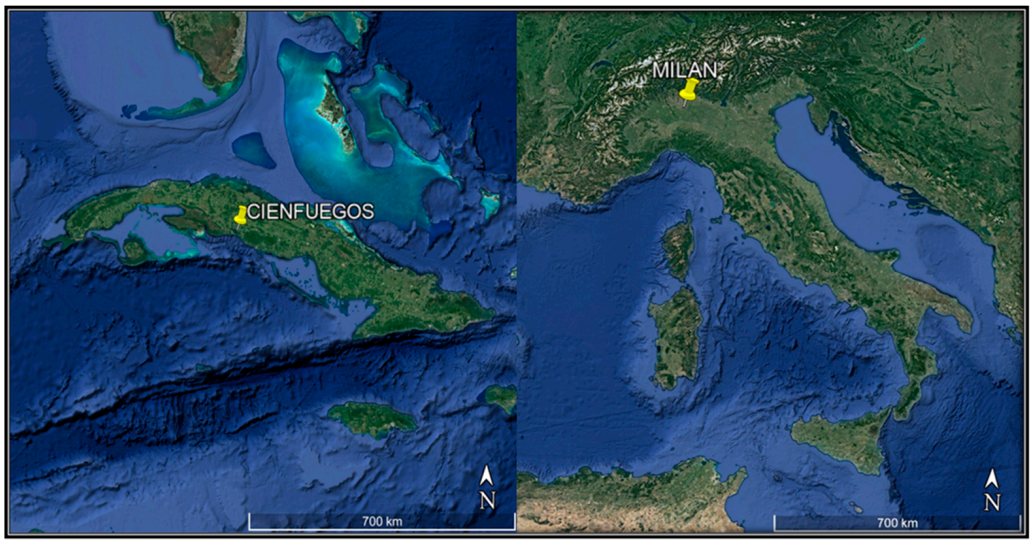

Figure 1. Position of the two sites in Italy and Cuba.

Both sites are mostly characterized by flat topography, typically agricultural land. To characterize the topography of the area, a reference is made to the SRTM1 dataset (Global—30 m) in both domains. For land use, the Corine CLC2018 dataset (Europe 100 m) is adopted for the Italian domain and Global Land Cover Characterization GLCC (Global—1 km) for the Cuban site, as there are no other data available in this region. Figure 2 reports the terrain elevations of the two simulation domains.

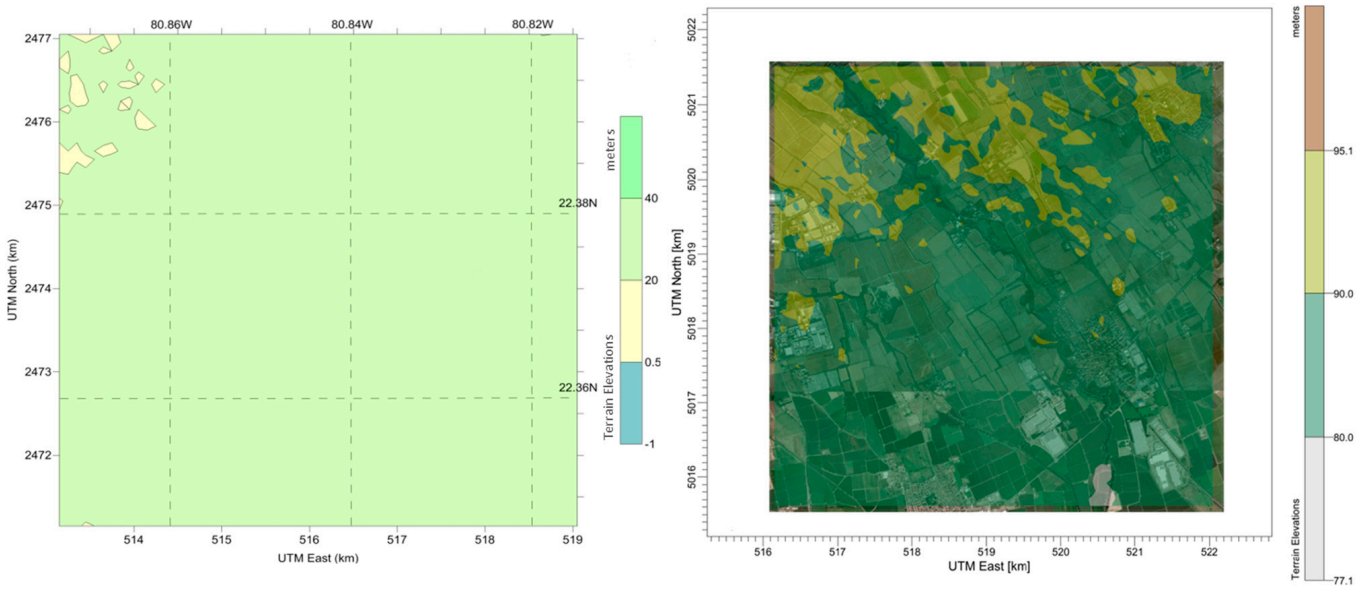

Figure 2. Terrain elevations for the Cuban domain (**left**) and Italian domain (**right**).

2.4. Emission Sources

To conclude the set of input variables required by the model, it is necessary to characterize the source term. Two different emission scenarios were hypothesized: the first, involving a point source (i.e., an odor emission abatement system); the second, an area source (i.e., a wastewater treatment tank). Both sources were positioned in the center of each simulation domain.

Characterization involves defining the geometrical parameters of the emission source as well as physical–chemical variables (e.g., temperature and velocity).

More specifically, for area sources, CALPUFF requires the definition of specific dimensional parameters: the dimension and height of the tank and the initial vertical dispersion coefficient, σ_{z0}, which identifies the puff's vertical dimension at emission. According to the US-EPA AERMOD User's Guide [48], σ_{z0} should be set by dividing the source's vertical dimension (i.e., height) by 2.15. This numerical coefficient is derived from the Gaussian distribution of the pollutant concentration inside the plume.

For point sources, it is necessary to define the geometrical dimensions of the emission (i.e., height and diameter), the temperature, and the velocity of the outlet gas.

Moreover, when considering odor emissions, it is crucial to specify the amount of odor emitted per unit time (Odor Emission Rate, OER), as discussed by Lucernoni [49]. Concerning emissions from area sources, the emissive parameter commonly referenced is the Specific Odor Emission Rate (SOER), i.e., the emission flow per square meter of the source. In addition, for area sources, as suggested by recent investigations [50,51], the odor emission rate was considered constant, as no hourly profile information is available, and it is not affected by wind velocity.

The parameters for the point and area sources are reported in Table 3. In both cases, no temporal variability of the emission is considered.

Table 3. Point and area source characterization.

Point Source		
Height	9	[m]
Diameter	1.2	[m]
Odor Emission Rate (OER)	2000	[ou_E/s]
Exit temperature	313	[K]
Exit velocity	5.4	[m/s]
Area Source		
Height	3	[m]
σ_{z0}	1.4	[m]
Odor Emission Rate (OER)	3500	[ou_E/s]
Specific Odor Emission Rate (SOER)	1.39	[$ou_E/m^2/s$]
Length X	42	[m]
Length Y	60	[m]

An additional parameter required to run the CALPUFF simulation is MDISP. It represents the method used to compute horizontal and vertical dispersion coefficients. As suggested by the US-EPA, a value of 2 was adopted for the MDISP parameter, which represents the calculation of turbulence-based dispersion coefficients from micrometeorological variables [40,42].

In addition to comparing the different odor impact maps resulting from the model runs, further evaluations were made by estimating the odor concentrations at a set of selected discrete receptors. A receptor nest was created by placing 324 receptors, radially separated by an angle of 20°, at distances of 50, 100, 150, 200, 400, 600, 800, 1000, 1200, 1400, 1600, 1800, 2000, 2200, 2400, 2600, 2800, and 3000 m from the source center, following the strategy outlined by [29].

In Table 4, below, the input parameters used in the simulations are summarized for both domains and for the different meteorological settings.

Table 4. Summary of input data for the simulations.

	NO-OBS		OBS		HYBRID	
	Italy	**Cuba**	**Italy**	**Cuba**	**Italy**	**Cuba**
Domain	6 km × 6 km (100 m mesh)	6 km × 6 km (100 m mesh)	6 km × 6 km (100 m mesh)	6 km × 6 km (100 m mesh)	6 km × 6 km (100 m mesh)	6 km × 6 km (100 m mesh)
Sources	Point + area	Point + area	Point + area	Point + area	Point + area	Point + area
Topographic data	SRTM1 (Global—30 m)	SRTM1 (Global—30 m)	SRTM1 (Global—30 m)	SRTM1 (Global—30 m)	SRTM1 (Global—30 m)	SRTM1 (Global—30 m)
Surface meteorological Data	WRF (1 km)	WRF (3 km)	Landriano Cascina Marianna Station (ARPA Lombardia)	Aguada de Pasajeros Station (Cienfuegos)	Landriano Cascina Marianna Station (ARPA Lombardia)	Aguada de Pasajeros Station (Cienfuegos)
Upper meteorological Data	WRF (1 km)	WRF (3 km)	NOAA/ESRL Radiosonde Database, (Milano Linate Airport)	Key West (Florida) upper air station	WRF (1 km)	WRF (3 km)

2.5. Statistical Metrics

Normalized Mean Bias (NMB) and FAC2 statistical indicators [52–55] are computed to compare CALPUFF results with the different input meteorological settings:

$$NMB_{1,2} = \frac{\sum_{i=1}^{N}(M_1 - M_2)}{\sum_{i=1}^{N} M_2} \qquad NMB_{2,3} = \frac{\sum_{i=1}^{N}(M_2 - M_3)}{\sum_{i=1}^{N} M_3} \qquad NMB_{1,3} = \frac{\sum_{i=1}^{N}(M_1 - M_3)}{\sum_{i=1}^{N} M_3} \tag{3}$$

$$FAC2_{1,2}{:}0.5 \leq \frac{M_1}{M_2} \leq 2 \qquad FAC2_{2,3}{:}0.5 \leq \frac{M_2}{M_3} \leq 2 \qquad FAC2_{1,3}{:}0.5 \leq \frac{M_1}{M_3} \leq 2 \tag{4}$$

where i identifies each discrete receptor, M is the single modeled concentration value, 1 = NO-OBS; 2 = OBS; 3 = HYBRID. NMB = 0 is the optimal value indicating the best fit between the different models. The FAC2 index, which stands for "Factor of 2", quantifies the percentage of data points for which the ratio between modeled and observed values falls within a specific range, typically defined as ±50% of the observed value. In other words, it measures how many modeled values are within a factor of 2 (i.e., between half and double) of the observed values. This index provides an indication of the model's ability to accurately predict the observed values within a certain tolerance level.

3. Results and Discussion

3.1. Wind Roses

Before delving into the discussion of the CALPUFF results, it is worthwhile to thoroughly examine the CALMET output generated under three distinct input meteorological settings: "NO-OBS", "OBS", and "HYBRID". Figure 3 depicts the wind roses in the first vertical layer (i.e., 10 m from the ground) extracted from the CALMET simulations, indicating the main directions from which the wind blows.

In Italy (left side), the graphs show that the prevailing winds are from the east (E) and west (W), with wind speeds that almost never exceed 10 m/s. In this case, the "NO-OBS" simulation seems to slightly overestimate the wind speed compared to the other simulations in the domain. As expected, the "OBS" and "HYBRID" simulations show the same wind rose in the first vertical layer. In fact, the hybrid simulation processes observed data from the surface station. "OBS" and "HYBRID" show a higher calm percentage compared to the "NO-OBS" simulation, i.e., 15.3% vs. 2.6%, with generally lower wind speeds, always below 9 m/s. Due to the lack of a unanimous definition of wind calm, for these simulations, calm conditions are defined as a wind speed lower than 0.5 m/s.

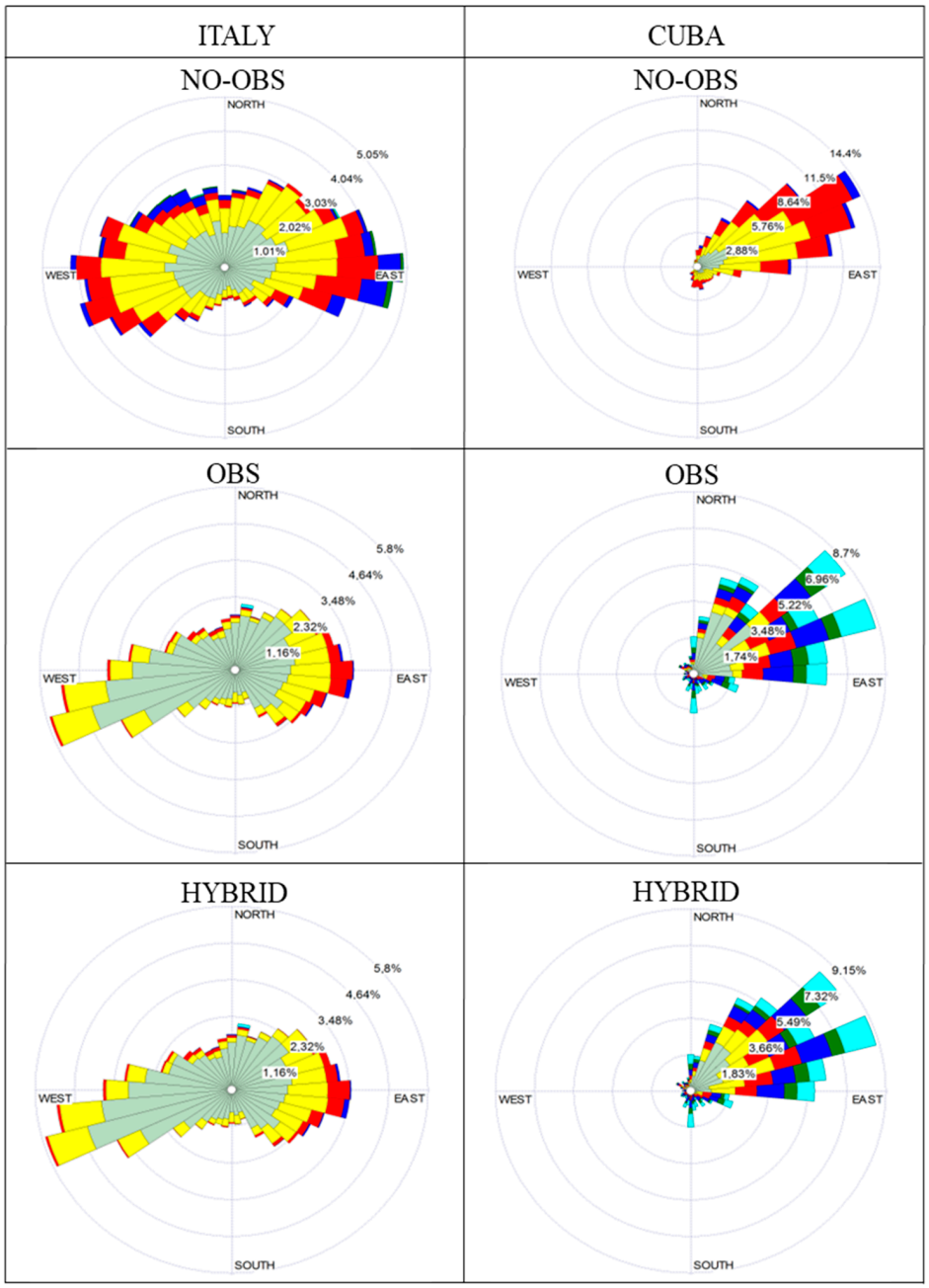

CALMS %	ITALY	CUBA
NO-OBS	2.6%	1.2%
OBS	15.3%	25.9%
HYBRID	15.3%	25.9%

Figure 3. Wind roses and calm percentage for Italy (**left**) and Cuba (**right**) for the year 2016, with the "NO-OBS", "OBS", and "HYBRID" models.

In Cuba (right side), the graphs show that the prevailing winds are from the northeast (NE), with wind speeds generally higher than in Italy. In this case, the "NO-OBS" simulation seems to slightly underestimate wind speed values in the domain compared to "OBS" and

"HYBRID", returning a calm percentage of 1.2%. The wind roses for "OBS" and "HYBRID" are not exactly identical, as seen in Italy, presumably due to the significant amount of invalid data (almost 20%) in the input dataset of the Cuban surface station and subsequent CALMET processing of missing input data. Nevertheless, CALMET roses returned from "OBS" and "HYBRID" simulations demonstrate a similar wind speed behavior, seemingly overestimating the wind speed compared to "NO-OBS", with values exceeding 11 m/s.

3.2. Contour Maps

Figures 4 and 5 show the simulated contour maps for the point source and the area source, respectively. In each of these graphs, the CALPUFF results on the Italian domain (top) and Cuban one (bottom) are compared by setting the three different CALMET input meteorological settings: from the left to the right, "NO-OBS", "OBS", and "HYBRID" simulations are reported. In addition, in the Supplementary Material, the odor concentration values (98th percentile on an annual basis) of discrete receptors are reported (Tables S1–S4).

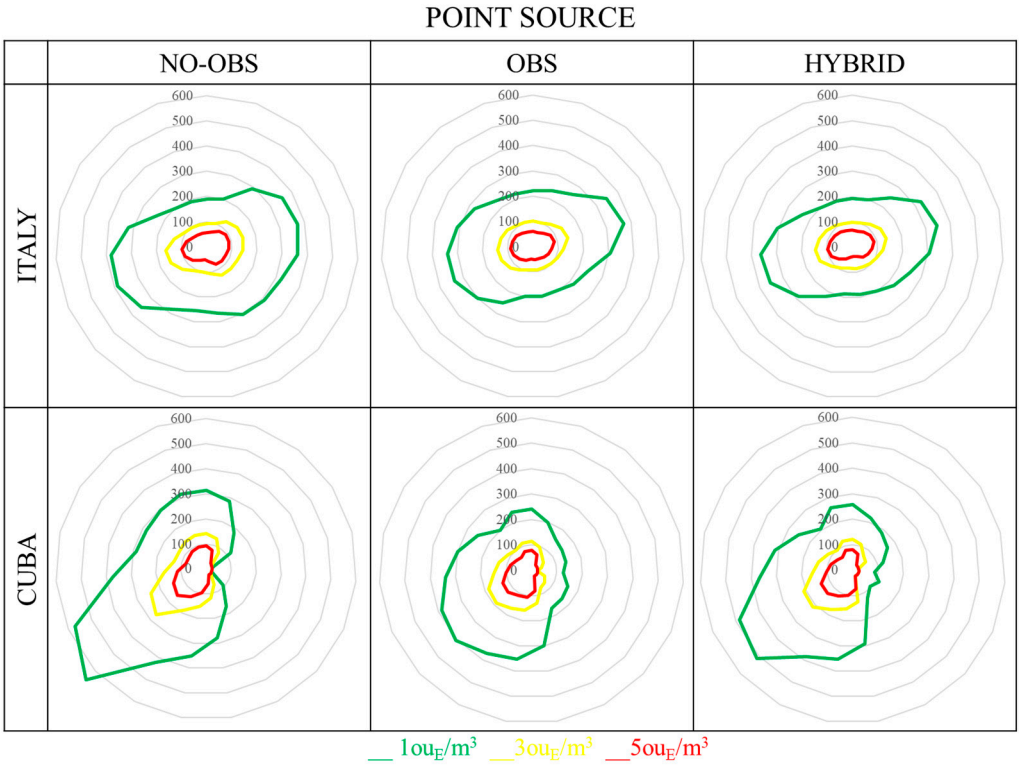

Figure 4. Contour maps for the point source site for all the simulations, highlighting the distances (m) from the emissions source. The (**upper**) maps show the Italian domain, while the (**lower**) maps consider the Cuban one.

According to the Italian Lombardy Region Guideline for odor [33], odor impact maps should incorporate three reference odor concentration values in ou_E (European odor unit): 1 ou_E/m^3, 3 ou_E/m^3, and 5 ou_E/m^3. These values correspond to:

- At 5 ou_E/m^3, 90–95% of the population perceives the odor.
- At 3 ou_E/m^3, 85% of the population perceives the odor.
- At 1 ou_E/m^3, 50% of the population perceives the odor.

The aforementioned guideline mandates the computation of the 98th percentile of odor peak concentration values on an annual basis. Despite the absence of a universal approach for defining short-term peak concentration, a constant factor of 2.3 is suggested [33]. Due to the lack of a technical standard for odor in Cuba, the aforementioned criterion has been considered in the current study for both the Cuban and Italian domains.

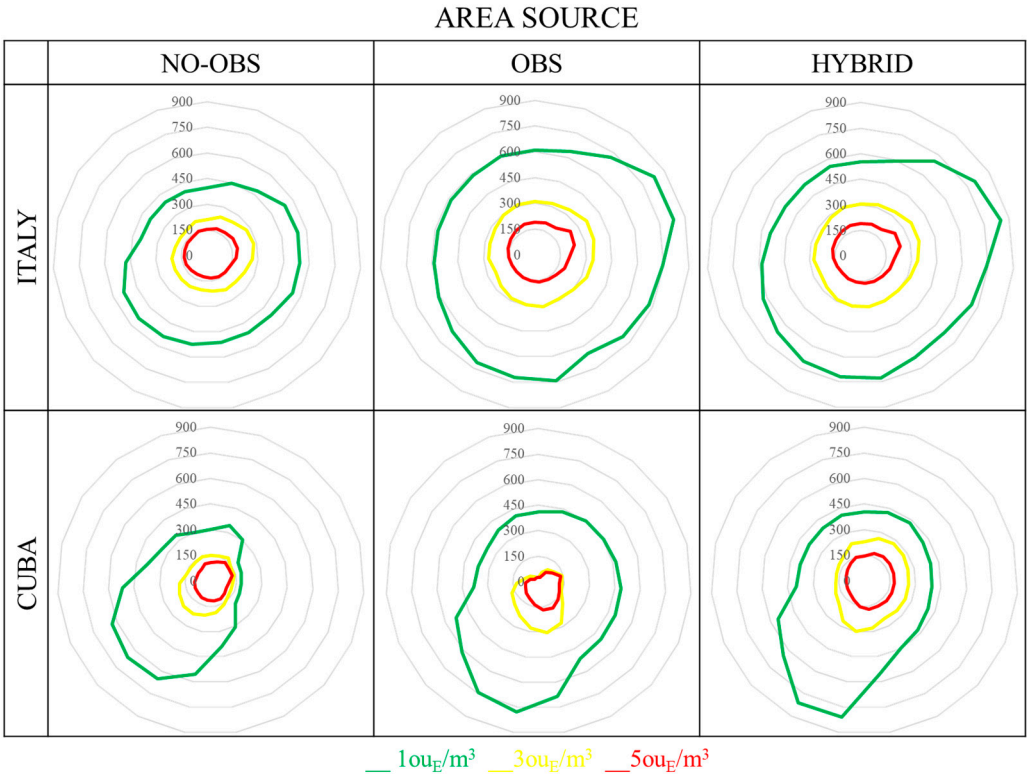

Figure 5. Contour maps for the area source site for all model simulations, highlighting the distances (m) from the emissions source. The (**upper**) maps show the Italian domain, while the (**lower**) maps consider the Cuban one.

Looking at the simulated contour maps for the point source (Figure 4), it is evident that, in the Italian site, the major impact is observed along the east (E) and west (W) directions, consistent with the prevailing wind directions shown in Figure 3.

Similarly, in the Cuban domain, the contour maps still exhibit odor impact coherent with the most frequently observed wind direction, i.e., southwest (SW).

In the Italian domain, the contour line corresponding to 5 ou$_E$/m^3 reaches a maximum distance of about 100 m along the prevailing wind directions (E and W). For 3 ou$_E$/m^3, the lines extend from 100 m to 200 m. Considering the distance related to 1 ou$_E$/m^3, the maximum value is 400 m in the main wind directions (E and W).

In the Cuban domain, the contour lines for 5 ou$_E$/m^3, 3 ou$_E$/m^3, and 1 ou$_E$/m^3 reach about 150 m, 300 m, and 600 m, respectively, along the prevailing wind direction (SW).

The most interesting outcome from this investigation is that in both domains, the "NO-OBS", "OBS", and "HYBRID" simulations are comparable in terms of odor impact.

Concerning the area source impact maps (Figure 5), in the Italian domain, the contour line corresponding to 5 ou$_E$/m^3 reaches a maximum distance of about 150 m for "NO-OBS" simulations and 250 m for the "OBS" and "HYBRID" modes in the main east direction. For 3 ou$_E$/m^3, the maximum distance is about 300 m for "NO-OBS" and 350 m for "OBS" and "HYBRID". Finally, considering the reference value of 1 ou$_E$/m^3, the line achieves a maximum distance of 500 m and 800 m for "NO-OBS" and "OBS"/"HYBRID", respectively.

In the Cuban domain, the line corresponding to 5 ou$_E$/m^3 reaches a distance of 150 m for "NO-OBS" and 200 m for the "OBS" and "HYBRID" mode. The distance for 3 ou$_E$/m^3 reaches 200 m for "NO-OBS" and 300 m in the other cases in the main SW direction. Finally, for the contour line corresponding to 1 ou$_E$/m^3, the maximum distance is 600 m and 800 m for NO-OBS and "OBS"/"HYBRID", respectively.

Overall, the results obtained with the three input meteorological settings appear comparable. However, the "OBS" and "HYBRID" simulations seem very similar, while "NO-OBS" slightly underestimates the odor impact compared to the other simulations.

For both the Cuban and Italian domains, the overestimation resulting from the "OBS" and "HYBRID" simulations compared to "NO-OBS" may be attributable to the higher percentage of wind calms, reported in Figure 3, which typically represents the worst situation for odor dispersion.

To summarize, contour maps simulated for the area source exhibit greater discrepancies compared to the point source when implementing different meteorological input data. This discrepancy could be attributed to variations in emissive and dispersion mechanisms, particularly characterized by plume rise (z) in the case of point sources, as estimated using the Briggs equation [34]:

$$z = \left[\frac{3F_m x}{\beta_j^2 u_s^2} + \frac{3Fx^2}{2\beta_1^2 u_s^3} \right]^{1/3} \quad (5)$$

where F_m [m^4/s^2] is the momentum flux, F [m^4/s^3] is the buoyancy flux, u_s [m/s] is the stack height wind speed, x [m] is the downwind distance, β_1 [-] is the neutral entrainment parameter, and β_j [-] is the jet entrainment parameter.

A possible explanation is that the temperature gradient between the emission and the atmosphere (which influences the buoyancy flux F) is the controlling phenomenon for pollutant dispersion and dilution. This may lead to a reduced impact of local meteorological conditions.

3.3. Separations Distances

Figure 6 illustrates, for both domains, the direction-dependent separation distances for the three reference concentration values specified in the Italian guidelines (i.e., 1 ou_E/m^3, 3 ou_E/m^3, 5 ou_E/m^3). These separation distances represent contour lines (isopleths), varying according to direction, of an ambient concentration threshold. The left graph refers to both point sources and the right graph to area source.

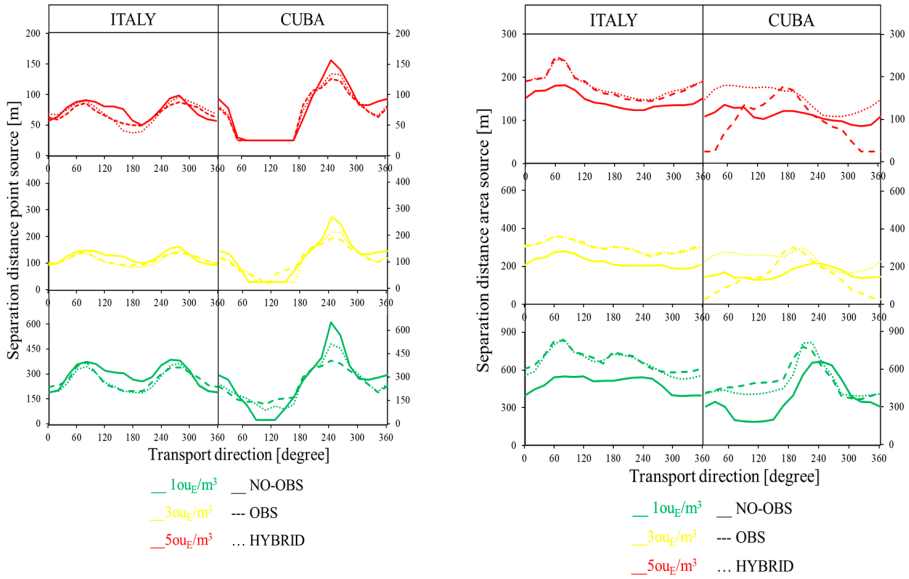

Figure 6. Direction-dependent separation distances considering the Italian domain and the Cuban one for the point source (**left** graph) and area source (**right** graph).

In very few cases, separation distances were found to be below 50 m, which is the distance of the first discrete receptor from the emission source. In such instances, a minimum separation distance of 25 m was considered.

First, focusing on the results of the point source, in the left part of Figure 6, the separation distances obtained for the Italian site (left) with the three different input meteorological settings appear almost overlapped. The same behavior is observed for the Cuban domain (right). In particular, for the "HYBRID" and "OBS" simulations, the lines are even closer,

overlapping in different sectors, with few discrepancies in the main direction of the wind, particularly in the SW direction in the Cuban domain.

The separation distance related to 5 ou_E/m^3 in the Italian domain achieves a maximum value of roughly 100 m along the prevalent wind directions (E and W). Lines for 3 ou_E/m^3 are relatively close, ranging from 100 m to 200 m. The greatest value in the main wind directions (E and W) is 400 m when the distance refers to 1 ou_E/m^3.

For the Cuban domain, the separation distance associated with 5 ou_E/m^3 reaches a maximum of about 150 m. Lines for 3 ou_E/m^3 reach 300 m, whereas lines for 1 ou_E/m^3 reach 600 m. All of these values are obtained along the predominant wind direction (SW).

In conclusion, as previously discussed for the odor contour maps, the point source impacts simulated with different meteorological input data appear largely comparable.

As observed in the discussion regarding odor impact maps, separation distances with different meteorological input data (Figure 6) exhibit greater discrepancies for both domains when simulated for area sources compared to point sources. Specifically, in the case of area sources, the lines tend to converge and overlap across different sectors in the "HYBRID" and "OBS" simulations, with some discrepancies noted in the Cuban domain, possibly attributable to a higher percentage of invalid data.

The separation distance of 5 ou_E/m^3 in the Italian domain achieves its greatest value in the main east direction at roughly 150 m for "NO-OBS" simulations and 250 m for the "OBS" and "HYBRID" modes. The separation distance for 3 ou_E/m^3 is approximately 300 m for "NO-OBS" and 400 m for "OBS" and "HYBRID". Finally, with a reference value of 1 ou_E/m^3, the maximum separation distances for "NO-OBS" and "OBS"/"HYBRID" are 500 m and 800 m, respectively.

Simulated separation distances for the "OBS" and "HYBRID" modes in the Cuban domain differ more with respect to the point source. The 5 ou_E/m^3 line has a range of 150 m for "NO-OBS" and 200 m for the "OBS" and "HYBRID" mode. In the major SW direction, the separation distance of 3 ou_E/m^3 is 200 m for "NO-OBS" and 300 m in the other situations. The maximum distance for lines with 1 ou_E/m^3 is, hence, 600 m for "NO-OBS" lines and 800 m for "OBS"/"HYBRID" lines, respectively.

In conclusion, in the case of the area source, as previously revealed by the odor impact maps, "NO-OBS" results appear slightly underestimated compared to the "OBS" and "HYBRID" simulation.

3.4. Statistical Metrics

NMB, as defined in Section 2.5, is computed for each combination of input meteorological data as a function of source distance. This is achieved by averaging the concentration values estimated on discrete receptors located at the same distance from the emission source (Figure 7).

Figure 7 confirms the optimal agreement between the "OBS" and "HYBRID" modes, with NMB values very close to 0. As can be noticed, particularly from the results obtained for the Italian domain, "NO-OBS" and "OBS" show the highest discrepancies. Furthermore, as discussed in the previous results, in the case of area sources, prognostic data appear to underestimate predicted concentrations compared to the "OBS" mode. On the other hand, for point sources, the "NO-OBS" mode seems to overestimate CALPUFF results compared to the "HYBRID" and "OBS" modes.

In the vicinity of the emission, the NMB indicator exhibits low values, with an increasing absolute value trend moving away from the source. This behavior suggests that similar results are achieved in close proximity to the emission source, regardless of the input meteorological settings. A possible explanation lies in the fact that the puffs, near the source, have not yet had time to move by advection, thus not experiencing the different meteorological fields. Conversely, at larger distances, meteorological data have a greater impact on CALPUFF outcomes.

The FAC2 statistical indicator, reported in Figure 8, reveals a very good agreement between the "OBS" and "HYBRID" modes, which decreases when introducing prognostic data. FAC2 index values for point sources are generally closer to the optimal value (i.e.,

100%, indicating the best fit between the two models) compared to area sources, as previously justified. In the case of point sources, FAC2 statistics are always higher than 70% (except for "NO-OBS"–"OBS", Cuba, with a percentage of 68%); for area sources, an FAC2 index of less than 60%, in a few cases, indicates a non-optimal agreement.

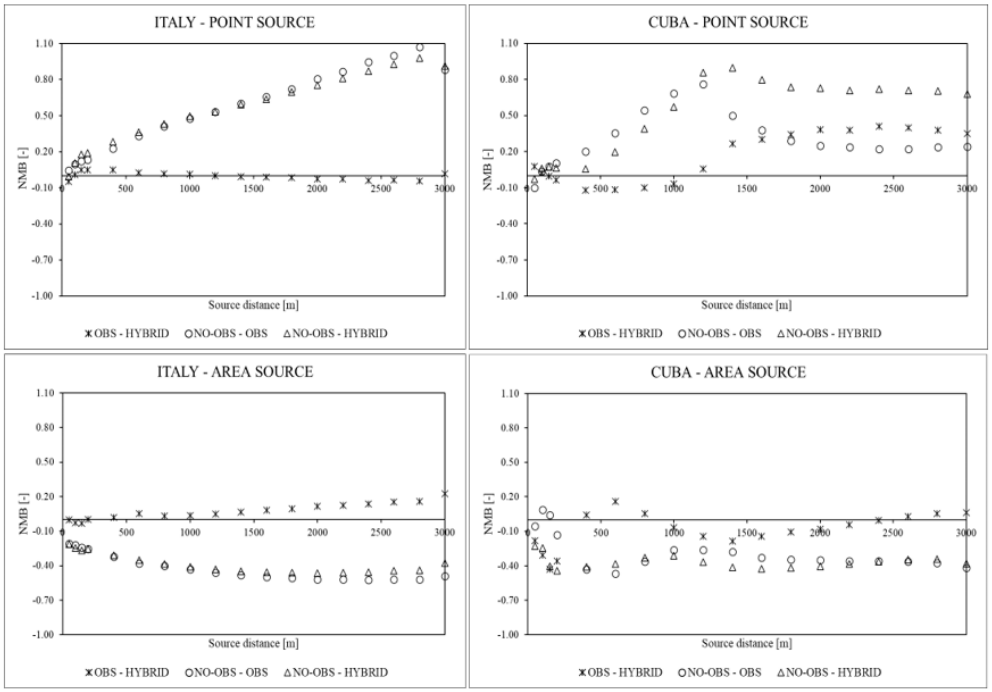

Figure 7. Normalized Mean Bias (NMB) as a function of source distance computed for the Italian (**left**) and Cuban (**right**) domain.

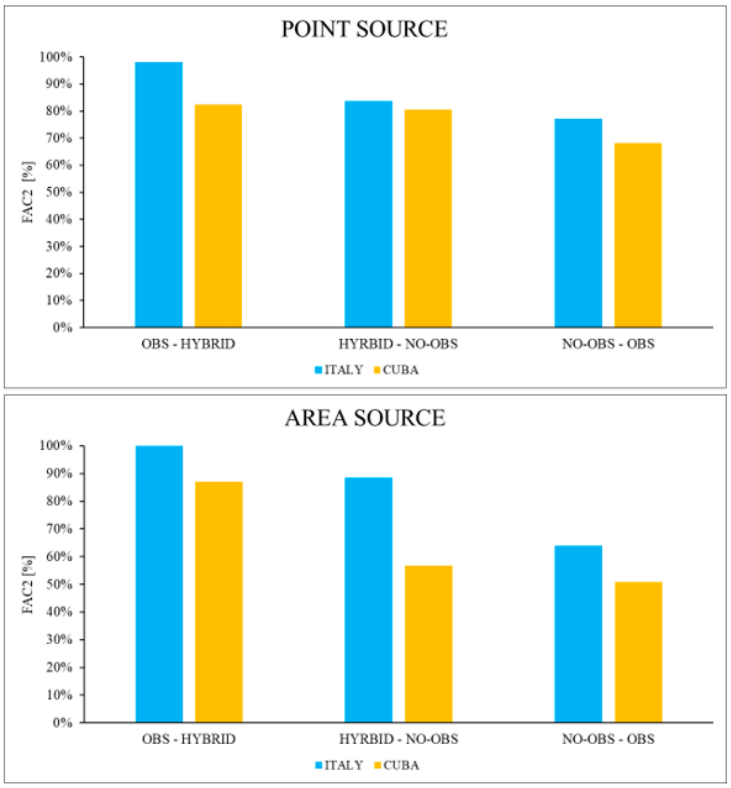

Figure 8. FAC2 index (%) for the different input meteorological settings. Point source (**upper**); area source (**down**).

Finally, from the comparison of the two simulation domains, it appears that estimated FAC2 index values are always lower in the Cuban domain. This is most likely due to the higher percentage of invalid meteorological data compared to the Italian station.

4. Conclusions

The present investigation provides information on how different input meteorological models may affect the results of odor dispersion modeling.

In this regard, the study focuses on comparing CALPUFF results by setting different CALMET input meteorological data: surface and upper air observational meteorological data ("OBS" mode), 3D prognostic meteorological data ("NO-OBS" mode), and blended prognostic and measured single station observational meteorological data ("HYBRID" mode). For the simulations, two different domains (northern Italy and Cuba) and two different types of emission sources were investigated.

The elaboration of the results refers to the odor impact criteria in force in some Italian regions by computing the 98th percentile of odor peak concentration values on an annual basis.

From the model results, it turns out that in the case of an area source, "OBS" and "HYBRID" simulations are very similar, while the "NO-OBS" mode slightly underestimates odor impact compared to the other simulations. For both Cuban and Italian domains, this evidence may be attributable to the lower percentage of wind calms in the "NO-OBS" mode.

On the contrary, for a point source, all the simulation runs, "NO-OBS", "OBS", and "HYBRID", are comparable in the Italian and Cuban domains. The different behavior, compared to an area source, may be due to the different emissive and dispersion mechanism, characterized by the plume rise in the case of a point source.

As previously mentioned, observational data from the Cuban meteorological station show a significant percentage of invalid data (i.e., almost 20%). Given the difficulty of running and maintaining the current network of Cuban weather stations, it is expected that the quality and the volume of data may be restricted.

To enhance and optimize the performance of the "NO-OBS" model, it may be helpful to implement additional surface stations in the same domain and investigate how to properly set the parameters R1 and R2 under these conditions.

Another crucial variable for the "NO-OBS" simulation is the cloud cover. Unfortunately, many surface stations do not directly provide this parameter. Several approaches, including theoretical ones, have been suggested in the literature for cloud cover estimation. Future research could investigate these approaches and assess CALPUFF's sensitivity to this variable.

As this work specifically focused on domains with flat orography, it would be interesting to evaluate different meteorological models in a complex orography domain since 3D reconstruction of wind fields is more difficult in non-flat terrain.

Finally, the present investigation provides information on how the WRF prognostic model can affect the conclusions of an odor impact assessment. Future research could explore alternative forecast models like MPAS, reanalysis data such as ERA5, or investigate techniques like nudging or data assimilation of observations within the WRF model.

Supplementary Materials: The following supporting information can be downloaded at: https://www.mdpi.com/article/10.3390/app14062457/s1, Table S1: Odor concentration values—98th percentile on annual basis for Point source (Italy); Table S2: Odor concentration values—98th percentile on annual basis for Point source (Cuba); Table S3: Odor concentration values—98th percentile on annual basis for Area source (Italy); Table S4: Odor concentration values—98th percentile on annual basis for Area source (Cuba).

Author Contributions: Conceptualization, F.T., L.F., M.I., A.H.-G. and S.S.; methodology, F.T., M.I. and A.H.-G.; software, F.T., L.F., A.L.F.H. and A.H.-G.; investigation, F.T., L.F., M.I. and A.H.-G.; data curation, F.T., M.I. and A.L.F.H.; visualization, F.T., M.I., A.L.F.H. and S.S.; writing—original draft, F.T.

and L.F.; writing—review and editing, M.I., A.H.-G. and S.S.; supervision, S.S. All authors have read and agreed to the published version of the manuscript.

Funding: This research received no external funding.

Institutional Review Board Statement: Not applicable.

Informed Consent Statement: Not applicable.

Data Availability Statement: The raw data supporting the conclusions of this article will be made available by the authors on request.

Conflicts of Interest: The authors declare no conflicts of interest.

References

1. García-Pérez, J.; de Larrea-Baz, N.F.; Lope, V.; Molina, A.J.; O'Callaghan-Gordo, C.; Alonso, M.H.; Rodríguez-Suárez, M.M.; Mirón-Pozo, B.; Alguacil, J.; Gómez-Acebo, I.; et al. Residential proximity to industrial pollution sources and colorectal cancer risk: A multicase-control study (MCC-Spain). *Environ. Int.* **2020**, *144*, 106055. [CrossRef]
2. Leogrande, S.; Alessandrini, E.R.; Stafoggia, M.; Morabito, A.; Nocioni, A.; Ancona, C.; Bisceglia, L.; Mataloni, F.; Giua, R.; Mincuzzi, A.; et al. Industrial air pollution and mortality in the Taranto area, Southern Italy: A difference-in-differences approach. *Environ. Int.* **2019**, *132*, 105030. [CrossRef]
3. Badach, J.; Kolasińska, P.; Paciorek, M.; Wojnowski, W.; Dymerski, T.; Gębicki, J.; Dymnicka, M.; Namieśnik, J. A case study of odour nuisance evaluation in the context of integrated urban planning. *J. Environ. Manag.* **2018**, *213*, 417–424. [CrossRef]
4. Brancher, M.; Griffiths, K.D.; Franco, D.; de Melo Lisboa, H. A review of odour impact criteria in selected countries around the world. *Chemosphere* **2017**, *168*, 1531–1570. [CrossRef] [PubMed]
5. Hawko, C.; Verriele, M.; Hucher, N.; Crunaire, S.; Leger, C.; Locoge, N.; Savary, G. A review of environmental odor quantification and qualification methods: The question of objectivity in sensory analysis. *Sci. Total Environ.* **2021**, *795*, 148862. [CrossRef] [PubMed]
6. Conti, C.; Guarino, M.; Bacenetti, J. Measurements techniques and models to assess odor annoyance: A review. *Environ. Int.* **2020**, *134*, 105261. [CrossRef] [PubMed]
7. Palmiotto, M.; Fattore, E.; Paiano, V.; Celeste, G.; Colombo, A.; Davoli, E. Influence of a municipal solid waste landfill in the surrounding environment: Toxicological risk and odor nuisance effects. *Environ. Int.* **2014**, *68*, 16–24. [CrossRef] [PubMed]
8. Piccardo, M.T.; Geretto, M.; Pulliero, A.; Izzotti, A. Odor emissions: A public health concern for health risk perception. *Environ. Res.* **2022**, *204*, 112121. [CrossRef] [PubMed]
9. Sironi, S. *Odour Regulation and Policies. Odour Impact Assessment Handbook*; John Wiley & Sons: Hoboken, NJ, USA, 2012.
10. Bokowa, A.; Diaz, C.; Koziel, J.A.; McGinley, M.; Barclay, J.; Schauberger, G.; Guillot, J.-M.; Sneath, R.; Capelli, L.; Zorich, V.; et al. Summary and overview of the odour regulationsworldwide. *Atmosphere* **2021**, *12*, 206. [CrossRef]
11. Cai, B.; Wang, J.; Long, Y.; Li, W.; Liu, J.; Ni, Z.; Bo, X.; Li, D.; Wang, J.; Chen, X.; et al. Evaluating the impact of odors from the 1955 landfills in China using a bottom-up approach. *J. Environ. Manag.* **2015**, *164*, 206–214. [CrossRef] [PubMed]
12. Dinçer, F.; Dinçer, F.K.; Sarı, D.; Ceylan, Ö.; Ercan, Ö. Dispersion modeling and air quality measurements to evaluate the odor impact of a wastewater treatment plant in İzmir. *Atmos. Pollut. Res.* **2020**, *11*, 2119–2125. [CrossRef]
13. Varela-Bruce, C.; Antileo, C. Assessment of odour emissions by the use of a dispersion model in the context of the proposed new law in Chile. *J. Environ. Manag.* **2021**, *295*, 113208. [CrossRef] [PubMed]
14. Barbulescu, A.; Barbes, L. Modeling the carbon monoxide dissipation in Timisoara, Romania. *J. Environ. Manag.* **2017**, *204*, 831–838. [CrossRef] [PubMed]
15. Dourado, H.; Santos, J.M.; Reis, N.C.; Mavroidis, I. Development of a fluctuating plume model for odour dispersion around buildings. *Atmos. Environ.* **2014**, *89*, 148–157. [CrossRef]
16. Geng, X.; Xie, Z.; Zhang, L. Influence of emission rate on atmospheric dispersion modeling of the Fukushima Daiichi Nuclear Power Plant accident. *Atmos. Pollut. Res.* **2017**, *8*, 439–445. [CrossRef]
17. Holnicki, P.; Kałuszko, A.; Trapp, W. An urban scale application and validation of the CALPUFF model. *Atmos. Pollut. Res.* **2016**, *7*, 393–402. [CrossRef]
18. Ionov, D.V.; Makarova, M.V.; Kostsov, V.S.; Foka, S.C. Assessment of the NO_X integral emission from the St. Petersburg megacity by means of mobile DOAS measurements combined with dispersion modelling. *Atmos. Pollut. Res.* **2022**, *13*, 101598. [CrossRef]
19. Lateb, M.; Meroney, R.N.; Yataghene, M.; Fellouah, H.; Saleh, F.; Boufadel, M.C. On the use of numerical modelling for near-field pollutant dispersion in urban environments—A review. *Environ. Pollut.* **2016**, *208*, 271–283. [CrossRef]
20. Li, R.; Yuan, J.; Li, X.; Zhao, S.; Lu, W.; Wang, H.; Zhao, Y. Health risk assessment of volatile organic compounds (VOCs) emitted from landfill working surface via dispersion simulation enhanced by probability analysis. *Environ. Pollut.* **2023**, *316*, 120535. [CrossRef]
21. Milazzo, M.F.; Ancione, G.; Lisi, R. Emissions of volatile organic compounds during the ship-loading of petroleum products: Dispersion modelling and environmental concerns. *J. Environ. Manag.* **2017**, *204*, 637–650. [CrossRef]

22. de Ferreyro Monticelli, D.; Santos, J.M.; Dourado, H.O.; Moreira, D.M.; Reis, N.C. Assessing particle dry deposition in an urban environment by using dispersion models. *Atmos. Pollut. Res.* **2020**, *11*, 1–10. [CrossRef]
23. Invernizzi, M.; Brancher, M.; Sironi, S.; Capelli, L.; Piringer, M.; Schauberger, G. Odour impact assessment by considering short-term ambient concentrations: A multi-model and two-site comparison. *Environ. Int.* **2020**, *144*, 105990. [CrossRef] [PubMed]
24. Dai, W.; Otto, C.; Reeves, D. Performing CALPUFF Analyses with Pseudo-Station Data Derived from MM5 Data. 2000. Available online: https://d3pcsg2wjq9izr.cloudfront.net/files/3783/articles/5161/tp_perform_calpuff.pdf (accessed on 13 May 2023).
25. Tagliaferri, F.; Invernizzi, M.; Capelli, L. A sensitivity analysis applied to SPRAY and CALPUFF models when simulating dispersion from industrial fires. *Atmos. Pollut. Res.* **2022**, *13*, 101249. [CrossRef]
26. Xu, H.; Zhu, Y.; Wang, L.; Lin, C.-J.; Jang, C.; Zhou, Q.; Yu, B.; Wang, S.; Xing, J.; Yu, L. Source contribution analysis of mercury deposition using an enhanced CALPUFF-Hg in the central Pearl River Delta, China. *Environ. Pollut.* **2019**, *250*, 1032–1043. [CrossRef] [PubMed]
27. Brancher, M.; Hieden, A.; Baumann-Stanzer, K.; Schauberger, G.; Piringer, M. Performance evaluation of approaches to predict sub-hourly peak odour concentrations. *Atmos. Environ. X* **2020**, *7*, 100076. [CrossRef]
28. Hernández-Garces, A.; Cécé, R.; Ferrer, A.; Bernard, D.; Jauregui-Haza, U.; Zahibo, N.; González, J.A. Intercomparison of FLEXPART and CALPUFF dispersion models. An application over a small tropical island. *Atmósfera* **2020**, *34*, 337–355. [CrossRef]
29. Tagliaferri, F.; Facagni, L.; Invernizzi, M.; Sironi, S. Variability in odour impact assessment due to different cloud cover estimation approaches: A northern Italy case study. *Case Stud. Chem. Environ. Eng.* **2023**, *8*, 100492. [CrossRef]
30. Mistry, M.N.; Schneider, R.; Masselot, P.; Royé, D.; Armstrong, B.; Kyselý, J.; Orru, H.; Sera, F.; Tong, S.; Lavigne, É.; et al. Comparison of weather station and climate reanalysis data for modelling temperature-related mortality. *Sci. Rep.* **2022**, *12*, 5178. [CrossRef]
31. Velázquez-Zapata, J.A. Comparing meteorological data sets in the evaluation of climate change impact on hydrological indicators: A case study on a Mexican basin. *Water* **2019**, *11*, 2110. [CrossRef]
32. Murguia, W.; Pagans, E.; Barclay, J.; Scire, J. Case study: A comparison of predicted Odour exposure levels in Barcelona using CALPUFF lite, CALPUFF NoObs and CALPUFF Hybrid model. *Chem. Eng. Trans.* **2014**, *40*, 31–36. [CrossRef]
33. Lombardia, D.G.R. n.IX/3018. Determinazioni Generali in Merito Alla Caratterizzazione delle Emissioni Gassose in Atmosfera Derivanti da Attività a Forte Impatto Odorigeno. 2012, pp. 18–49. Available online: https://www.regione.lombardia.it/wps/wcm/connect/1008c34a-79b9-4185-8557-6ffd65eb7e86/DGR+3018_2012.pdf?MOD=AJPERES&CACHEID=ROOTWORKSPACE-1008c34a-79b9-4185-8557-6ffd65eb7e86-nK1Rz2t (accessed on 13 May 2023).
34. Scire, J.S.; Strimaitis, D.G.; Yamartino, R.J. *A User's Guide for the CALPUFF Dispersion Model*; Earth Tech, Inc.: Concord, MA, USA, January 2000; p. 521. Available online: http://www.src.com/calpuff/download/CALPUFF_UsersGuide.pdf (accessed on 17 April 2023).
35. US-EPA. Meteorological Monitoring Guidance for Regulatory Modeling Applications; Epa-454/R-99-005. 2000; p. 171. Available online: http://www.epa.gov/scram001/guidance/met/mmgrma.pdf (accessed on 15 April 2023).
36. US-EPA. Appendix W: Revisions to the Guideline on Air Quality Models: Enhancements to the AERMOD Dispersion Modeling System and Incorporation of Approaches to Address Ozone and Fine Particulate Matter. 2017. Available online: https://www.federalregister.gov/documents/2017/01/17/2016-31747/revisions-to-the-guideline-on-air-quality-models-enhancements-to-the-aermod-dispersion-modeling (accessed on 15 March 2023).
37. Rzeszutek, M. Parameterization and evaluation of the CALMET/CALPUFF model system in near-field and complex terrain–Terrain data, grid resolution and terrain adjustment method. *Sci. Total Environ.* **2019**, *689*, 31–46. [CrossRef]
38. Scire, J.; Robe, F.; Fernau, M.; Yamartino, R. *A User's Guide for the CALMET Meteorological Model*; Earth Tech, Inc.: Concord, MA, USA, 2000.
39. Rood, A.S. Performance evaluation of AERMOD, CALPUFF, and legacy air dispersion models using the Winter Validation Tracer Study dataset. *Atmos. Environ.* **2014**, *89*, 707–720. [CrossRef]
40. Varela, A.; Carnesoltas, M. Condiciones que favorecen el desarrollo de tornados en las provincias occidentales de Cuba en los períodos lluvioso y poco lluvioso. *Rev. Cuba. De Meteorol.* **2017**, *23*, 312–327.
41. Roque, A.; Pérez, D.; Rivero, I.; Muñiz, L.; Báez, R. Estudio del contenido integral del vapor de agua en la zona tropical comprendida entre los 17? y 25? latitud norte y los 66? y 97? longitud oeste. *Rev. Cuba. De Meteorol.* **2002**, *9*, 3–11.
42. Gandin, L.S. *The Planning of Meteorological Station Networks*; WMO Technical Note: Geneva, Switzerland, 2017.
43. Kitchen, M. Representativeness errors for radiosonde observations. *Q. J. R. Meteorol. Soc.* **1989**, *115*, 673–700. [CrossRef]
44. US-EPA. *Documentation of the Evaluation of CALPUFF and Other Long Range Transport Models Using Tracer Field Experiment Data*; ENVIRON International Corporation: Novato, CA, USA, 2012; pp. 1–147. Available online: http://www.epa.gov/scram001/reports/EPA-454_R-12-003.pdf (accessed on 12 February 2023).
45. Hernández-Garces, A.; González, J.A.; Casares, J.; Turtos, L.; Alvarez, L.; Jauregui-Haza, U. Caso de estudio en la bahía de jagua al sur de Cuba mediante un acoplamiento WRF/CALMET. *Rev. Bras. Meteorol.* **2017**, *32*, 659–667. [CrossRef]
46. The, J.L.; Lee, R.F. The Effect of the CALMET Surface Layer Weighting Parameter R1 on the Accuracy of CALMET at Other Nearby Sites: A Case Stud. 2003. Available online: https://citeseerx.ist.psu.edu/document?repid=rep1&type=pdf&doi=5765d4a68fa1c3038a71d47e194fd88412e2a5a3 (accessed on 17 April 2023).
47. Dresser, A.L.; Huizer, R.D. CALPUFF and AERMOD model validation study in the near field: Martins Creek revisited. *J. Air Waste Manag. Assoc.* **2011**, *61*, 647–659. [CrossRef] [PubMed]

48. US-EPA. *User's Guide for the AMS/EPA Regulatory Model (AERMOD)*; Epa-454/B-18-001; Air Quality Assessment Division: Research Triangle Park, NC, USA, 2018; Volume EPA-454/B-, pp. 1–137. Available online: http://www.epa.gov/scram001/7thconf/aermod/aermodugb.pdf (accessed on 5 March 2023).
49. Lucernoni, F. The evaluation of the Odour Emission Rate for passive area sources: A new approach. *Chem. Eng. Trans.* **2015**, *43*, 2149–2154. [CrossRef]
50. Tagliaferri, F.; Invernizzi, M.; Sironi, S. Experimental evaluation on liquid area sources: Influence of wind velocity and temperature on the wind tunnel sampling of VOCs emissions from wastewater treatment plants. *Chemosphere* **2023**, *312*, 137337. [CrossRef]
51. Tagliaferri, F.; Invernizzi, M.; Sironi, S. Influence of wind velocity on the emission rate of acetone aqueous solution at different concentrations. *Chem. Eng. Trans.* **2021**, *12*, 5178. [CrossRef]
52. Gustafson, W.I.; Yu, S. Generalized approach for using unbiased symmetric metrics with negative values: Normalized mean bias factor and normalized mean absolute error factor. *Atmos. Sci. Lett.* **2012**, *13*, 262–267. [CrossRef]
53. Hanna, S.; Chang, J. Skyscraper rooftop tracer concentration observations in Manhattan and comparisons with urban dispersion models. *Atmos. Environ.* **2015**, *106*, 215–222. [CrossRef]
54. Chang, J.C.; Hanna, S.R. Air quality model performance evaluation. *Meteorol. Atmos. Phys.* **2004**, *87*, 167–196. [CrossRef]
55. Willmott, C.J. On the validation of models. *Phys. Geogr.* **1981**, *2*, 184–194. [CrossRef]